Plasticity and Cytokinetic Dynamics of the Hair Follicle Mesenchyme: Implications for Hair Growth Control

Desmond J. Tobin, Andrei Gunin,* Markus Magerl, Bori Handijski,† and Ralf Paus†

Department of Biomedical Sciences, University of Bradford, Bradford, UK; *Department of Histology, Chuvash State University, Cheboksary, Russia; †Department of Dermatology, University Hospital Eppendorf, University of Hamburg, Hamburg, Germany

The continuously remodeled hair follicle is a uniquely exploitable epithelial-mesenchymal interaction system. In contrast to the cyclical fate of the hair follicle epithelium, the dynamics of the supposedly stable hair follicle mesenchyme remains enigmatic. Here we address this issue using the C57BL/6 hair research model.

During hair growth, increase in total follicular papilla size was associated with doubling of papilla cell numbers, much of which occurred *before* intra-follicular papilla cell proliferation, and subsequent to mitosis in the proximal connective tissue sheath. This indicates that some papilla cells originate in, and migrate from, the proliferating pool of connective tissue sheath fibroblasts. Follicular papilla cell number and total papilla size were maximal by anagen VI, but intriguingly, decreased by 25% during this period of sustained hair production. This cell loss, which continued during catagen, was not associated with intra-follicular papilla apoptosis, strongly indicating that fibroblasts migrate out of the late anagen/early catagen papilla and re-enter the proximal connective tissue sheath. Low-level apoptosis occurred only here, along with the "detachment" of cells from the regressing connective tissue sheath.

Thus, the hair follicle mesenchyme exhibits significant hair cycle-associated plasticity. Modulation of these cell interchanges is likely to be important during clinically important hair follicle transformations, e.g. vellus-to-terminal and terminal-to-vellus during androgenetic alopecia. ***Key words: apoptosis/connective tissue sheath/electron microscopy/dermal papilla/follicular–papilla/histomorphometry, proliferation. J Invest Dermatol 120:895–904, 2003***

Complex interactions between ectodermal and mesodermal components of the hair follicle result in the elaboration of five or six concentric cylinders of at least 15 distinct interacting cell subpopulations. These together produce a truly exceptional mini-organ (Paus and Cotsarelis, 1999) that rivals the vertebrate limb bud (Schaller *et al*, 2001) as a model for studies of the genetic regulation of morphogenesis (Philpott and Paus, 1998; Cotsarelis and Millar, 2001). The hair follicle is unique in the adult mammalian body in experiencing multiple and life-long recapitulations of its embryogenesis whenever it enters into its active growth stage (anagen) (Paus *et al*, 1999; Stenn and Paus, 2001). Critical to the control of this cyclical behavior are the follicular papilla (FP) and connective tissue sheath (CTS), which together form the hair follicle's mesenchymal compartments (Jahoda and Reynolds, 1996).

Previous studies have convincingly demonstrated that FP fibroblasts, and the morphogens they secrete, are critical in hair growth induction (anagen) (Cohen, 1961; Oliver, 1967; Jahoda *et al*, 1984; Reynolds *et al*, 1991; Robinson *et al*, 2001). Moreover, these components are critical for determining the developmental pathways of the overlying ectodermal cell lineages during hair follicle morphogenesis and cycling (Philpott and Paus, 1998; Matsuzaki and Yoshizato, 1998; Kishimoto *et al*, 2000; Lindner *et al*, 2000; Langbein *et al*, 2001), as long as close FP–epithelial contact is maintained (Link *et al*, 1990; Jahoda and Reynolds, 1996). Where this collapses, e.g., in the absence of a functional *hr* gene product, hair growth is aborted and the hair follicle degenerates (Panteleyev *et al*, 1998).

A positive linear relationship has long been recognized to exist between FP volume and hair caliber (Van Scott and Ekel, 1958): the volumetric ratio of FP cells (and their secretory activity) to hair matrix keratinocytes is crucially important for determining the size of the hair shaft produced. Additionally, the caliber of the hair shaft can also vary along its length, i.e., fine distal tip, thick mid region, and narrow proximal "club" end (Hutchinson and Thompson, 1997). Thus, this FP/matrix volumetric ratio is likely to change not only between the main stages of the hair cycle, but also during the substages of anagen, as in wool follicles (Ibrahim and Wright, 1982). Studying changes in FP volume and cell number can be expected to provide crucial information on changes in the secretory activity of the FP that underlie all hair follicle transformations during hair follicle cycling, vellus-to-terminal/terminal-to-vellus hair transformation events and changes in the hair shaft diameter, length, and pigmentation (Jahoda and Reynolds, 1996; Jahoda, 1998; Paus *et al*, 1999; Stenn and Paus, 2001).

The prevailing consensus in FP cell biology is that the hair follicle mesenchyme represents a very stable cell population with very little if any proliferative activity (Pierard and de la Brassinne, 1975; Jahoda, 1998). This view is supported more recently by the observation that the FP fibroblasts do not undergo apoptosis during hair follicle regression (catagen) (Weedon and Strutton, 1981; Lindner *et al*, 1997; Stenn *et al*, 1994) as they may be protected from apoptosis via permanent expression of high levels of the anti-apoptotic protein Bcl-2 (Stenn *et al*, 1994; Lindner *et al*,

Manuscript received May 27, 2003; revised January 6, 2003; accepted for publication January 9, 2003

Reprint requests to: Prof. Ralf Paus, Department of Dermatology, University Hospital, Eppendorf, University of Hamburg, Martinistr 52, Hamburg, Germany; Email: paus@uke.uni-hamburg.de

0022-202X/03/$15.00 ·

1997). There is, however, substantial clinical evidence that the FP is not static throughout life. This can be easily appreciated from the dramatic increases in FP size and cell number during puberty-associated vellus-to-terminal hair transformation (Barth 1987), hirsutism, and hypertrichosis, and vice versa during androgenetic alopecia development (Ishino *et al*, 1997).

Although androgens appear to play a major part, the underlying mechanisms involved in these hair follicle transformations are unclear. In particular, convincing explanations for an increase in FP cell number during the growth phase of the hair cycle have, for the most part, not been found in murine proliferation studies (Wessells and Roessner, 1965; Ibrahim and Wright, 1982; Tezuka *et al*, 1991). By contrast, FP cell proliferation has been reported in the primary sheep wool hair follicle (Adelson and Kelley, 1992) and in rat pelage follicles (Pierard and de la Brassinne, 1975). It remained unclear, however, whether this intrapapillary cell proliferation indeed reflected proliferating fibroblasts, as other potential sources of cell division include the endothelium of intrapapillary capillaries (Pierard and de la Brassinne, 1975).

In contrast to the FP, the relative contribution of the follicular CTS to hair growth control has only rather recently become systematically investigated (Reynolds *et al*, 1991; Jahoda *et al*, 1991; Horne and Jahoda, 1992; Matsuzaki *et al*, 1996; Jahoda, 1998). Early indication of a fundamental interaction between these two mesenchymal components of the hair follicle was convincingly demonstrated by the reformation of a FP from the lower CTS (Oliver 1967), indicating that significant plasticity exists within these two hair follicle fibroblast subpopulations, at least under conditions of experimental manipulation/trauma. Cell renewal in the CTS is also thought to be a very rare event. Indeed, the number of resident fibroblasts has been claimed to remain constant during the entire hair growth cycle (Pierard and de la Brassinne, 1975). Despite the marked hair growth cycle-dependent changes in hair follicle epithelial and mesenchymal cellularity (Parakkal, 1990; Jahoda *et al*, 1992) there is no consensus on the actual mechanism of CTS regression, including the fate of its cells and basal lamina/glassy membrane (Montagna and Parakkal, 1974).

On this background, we have employed the most comprehensively studied animal model in hair research, the C57BL/6 mouse (Paus *et al*, 1990), and have used both the depilation-induced and the spontaneous murine hair cycle to analyze systematically the plasticity and dynamics of the FP and CTS during hair follicle cycling. Another important advantage of using this model is that the absence of capillaries in their pelage FP (Durward and Rudall 1958) avoids the ambiguity affecting the interpretation of proliferating cells in the vascularized human hair follicle. The following specific questions were addressed: (i) What drives the reconstruction of the hair follicle mesenchyme during early anagen? (ii) Is the anagen-associated increase in FP size due to cell proliferation, cell migration, cell growth, and/or increases in production of extracellular matrix (ECM)? (iii) How does the reconstructing hair follicle epithelium influence the organization of the hair follicle mesenchyme during anagen development? (iv) Does regression of the hair follicle mesenchyme during catagen involve FP cell emigration to the CTS, loss of FP cell synthetic activity, and/or mesenchymal cell death? The questions were addressed by histomorphometric analyses of a range of proliferation markers, and planimetric analysis of changes in FP size, cell volume, and cell number. Cellular activity was examined using high-resolution light microscopy and transmission electron microscopy (TEM).

MATERIALS AND METHODS

Animals Female syngeneic C57BL/6 mice (Charles River, Sulzfeld, Germany) were used that had all back skin hair follicles in either the resting phase of the hair cycle (telogen; 6–9 wk of age) or had hair follicles that had just entered the first true cycle (anagen; postpartum day 28) after having completed hair follicle morphogenesis (Paus *et al*, 1999; Müller-Röver *et al*, 2001). The animals were housed in community cages with 12 h light periods, and were fed water and mouse chow *ad libitum*.

Hair follicle cycling was synchronized by wax/rosin depilation to obtain large numbers of hair follicles in the same hair cycle stage as previously described (Paus *et al*, 1990). Back skin was harvested on days 0, 1, 3, 5, 8, 12, 14, 15, 16, 17, 18, 19, 20, 25, and 34 postdepilation. In this way tissue was collected that contained hair follicles as they passed through one hair cycle from telogen (resting phase) to the start of hair regrowth (anagen I), via active hair shaft production (anagen IV–VI), through apoptosis-driven hair follicle regression (catagen), back to telogen (Müller-Röver *et al*, 2001). Immediately upon removal, the tissue was divided; part snap frozen and acetone fixed for Ki67 and proliferating cell nuclear antigen (PCNA) immunohistochemistry (Magerl *et al*, 2001) and part fixed in Karnovsky's fixative for high-resolution light microscopy and electron microscopy (Tobin *et al*, 1998). Skin treated with bromodeoxyuridine (BrdU) and colchicine (see below) for the assessment of mitotic indices was prepared as for Ki67 and PCNA.

In addition, back skin of 28 d old neonatal mice was harvested tissue and was assessed by high-resolution light microscopy and TEM as described bellow. This tissue contains hair follicles passing from the end of morphogenesis to the start of hair regrowth (anagen I), i.e., entering the first true anagen phase of the first cycle, and so facilitated a direct comparison between depilation-induced and spontaneous anagen. All animal studies were performed as approved by the responsible government institution, Berlin.

Assessment of cytokinetics

Ki67 and PCNA immunohistochemistry Cell proliferation was assessed via the immunohistochemical detection of two proliferation-associated proteins. Seven micrometer paraffin-embedded sections were incubated with the proliferation marker antibodies. The monoclonal antibody Ki67 (Dianova, GmbH, Hamburg, Germany) was employed to detect a 345–395 kDa protein complex expressed primarily during the S, G_2, and M phases of the cell cycle. Additionally, a monoclonal antibody to PCNA (Santa Cruz Biotechnology, Santa Cruz, CA, USA) was used to detect an auxiliary protein to DNA polymerase (present in cycling cells and most abundant during S phase. Following primary antibody incubations, sections were treated with peroxidase-labeled secondary antibody (Jackson Immuno-Research Labs, Inc., West Grove, PA, USA) and developed using 3,3′-diaminobenzidine-tetrachloride chromogen as previously described (Magerl *et al*, 2001).

BrdU incorporation Cell proliferation was further assessed by BrdU incorporation into cycling hair follicle cells to identify adequately cells in the S phase of the cell cycle, as previously described (Tezuka *et al*, 1991). Briefly, mice were injected intraperitoneally with BrdU (Sigma-Aldrich Chemie GmbH, Munich, Germany) dissolved in saline (20 microgram/g BW) 3 h before being killed. Harvested tissue was fixed in 4% formaldehyde and paraffin embedded. BrdU incorporation during S phase was examined immunohistochemically using anti-BrdU antibody (Santa Cruz), and alkaline phosphatase secondary antibody (Jackson Immuno-Research Labs). Color was developed with naphthol AS-BI phosphate/new fuchsin and hematoxylin as counterstain.

Mitotic Index In order to identify and quantify cells in the M phase of the cell cycle, selected mice were injected with colchicine (0.1 mg in 250 μl saline) 3 h before euthanasia. Thereafter, skin specimens were fixed and processed as above, counter-stained with Weigert's iron hematoxylin (for highlighting mitotic figures), and the number of cells with visible, colchicine-arrested, mitotic spindles counted in the hair follicle mesenchyme.

Apoptosis Incidence of apoptosis was assessed using classical morphologic criteria by both high-resolution light microscopy and TEM (Magerl *et al*, 2001). This was systematically compared with previously published results on mesenchymal cell apoptosis using the TUNEL (terminal deoxynucleotidyl transferase-mediated deoxyuridine triphosphate nick end-labeling) technique (Lindner *et al* 1997; Magerl *et al*, 2001).

High resolution light microscopy Representative tissue samples of skin from three mice at each of the test days above and from three p28 (postpartum day 28) mice were fixed in Karnovsky's fixative, post-fixed in 2% osmium tetroxide and uranyl acetate, and embedded in resin as previously described (Tobin *et al*, 1998). Semithin and ultrathin sections were cut with a Reichart-Jung microtome (Leica GmbH, Wetzlar, Germany); the former were stained with the metachromatic stain, toluidine blue/borax, examined by light microscopy and photographed (Leitz, Germany). Ultrathin sections were stained with uranyl acetate and lead citrate and were examined and photographed using a JEM-1200EX (Jeol, Tokyo, Japan). electron microscope.

Histomorphometry For quantitative histomorphometry, the hair follicle mesenchyme was divided into two defined subcompartments: the entire FP, and the proximal CTS. PCNA, Ki67, and BrdU proliferation indices were calculated as the number of labeled cells per 100 cells. The mitotic index was calculated in colchicine-treated specimens as a percentage of mitotic cells (anaphase to telophase) per total cells in the hair follicle compartment under view. In all cases, no less than 1000 cells in CTS were viewed per mouse. Twenty hair follicles in each of three blocks from three mice and at all time points were examined by light microscopy (i.e., total 2880 hair follicles). Five hair follicles from each block from each of three mice were examined by TEM at each test day (i.e., total 720 hair follicles).

Statistical analysis Arithmetic means and standard error of the mean were calculated. Statistical comparisons were performed with one-way analysis of variance and *post-hoc* Tukey's test (Statistica 5.0, StatSoft Inc.).

RESULTS

The proximal CTS appears to drive the reconstruction of the hair follicle mesenchyme during early anagen Cells located in the proximal CTS of telogen hair follicle undergo an abrupt and dramatic re-entry into the cell cycle approximately 1 d after anagen induction by depilation (**Fig 1*a***). As early as anagen I/II, up to 12% of cells in this component of the hair follicle mesenchyme are proliferating. By contrast, no proliferating cells were detected within the FP at this time. As anagen development progressed, the mitotic index in the proximal CTS peaked at 30%, whereas the mitotic index within the FP was never above 5% (**Fig 1*b***). Thus, a significant proportion of CTS cells entered the cell cycle a full 2 d before—a much more limited—cell division occurred in the FP (**Fig 1*b***). Despite this disparity in relative cell proliferation rates, however, total FP cell numbers increased significantly during early anagen development, and did so well before low level intra-FP cell proliferation was detectable (**Fig 2*a***). These findings strongly suggest that the increase in FP cell numbers during early anagen occurs largely via the immigration of cells from the proximal CTS into the FP.

Anagen development is associated with CTS cell proliferation and migration into the FP followed by local intra-FP cell proliferation Morphologic analysis can yield instructive, albeit static, glimpses, of the actual cellular dynamics involved in critical stages of the cycle. In addition to the above cytokinetic changes in the hair follicle mesenchyme during anagen development (**Figs 1*a,b* and 2**), evidence of CTS cell migration into the FP was also suggested by planimetric and histomorphologic analysis in both depilation-induced and spontaneous anagen development. Whereas a higher level of BrdU-positive cells, and a much higher mitotic index, were detected in the CTS than in the FP (**Figs 1, 3*b*, and 4*b***), this study still found that intra-FP cell proliferation can occur during anagen development (**Figs 3*j* and 4*a–c,e,f***). Interestingly, these cells were detected among attenuated CTS-like cells (**Figs 3*j* and 4*a***), as well as among more typical FP fibroblasts (**Fig 4*b,c,e,f***). This morphologic duality reflected a general tendency for the FP cell population to become increasingly heterogeneous during anagen I/II. Both oval FP cells and more attenuated CTS-like fibroblasts admixed in early anagen FP (**Figs 3*j* and 4*a***). Importantly, cells at the periphery of the FP were aligned parallel to the hair growth direction and assumed a more typical CTS attenuated form (**Fig 3*h***).

The source of fibroblasts that populate the growing CTS during anagen development is currently unknown. As the new hair follicle lengthened during anagen development, however, "free" mesenchymal cells were observed at proximal margins of the growing hair follicle (**Fig 3*i***). Whereas it was not possible to discern whether these cells were pre-CTS fibroblasts, they appeared to be more than randomly associated with the hair follicle, especially in the acellular mid and distal regions.

The increase in FP size during anagen development is due to a combination of increased cell number, increased cell size, and increased production of ECM The significant increase in total FP size during anagen development (**Fig 2*b***) is due not only to increased cell numbers (**Fig 2*a***) but also occurs via the growth of individual FP cells and increased production of ECM (**Fig 2*c***). Whereas FP cell number increased 2-fold from telogen to anagen, total FP size increased by more than 40-fold over telogen values (**Fig 2*b***). Anagen FP cells exhibited increased size associated with increases in a cytoplasmic to nuclear ratio, and increased nuclear euchromatism (this is indicative of a substantial increase in gene transcription (Wolffe and Guschin, 2000) and ovality (**Figs 3*g* and 4*a*** *vs* **Fig 5*a***). Whereas the exact contribution of ECM to the total volume of the anagen FP

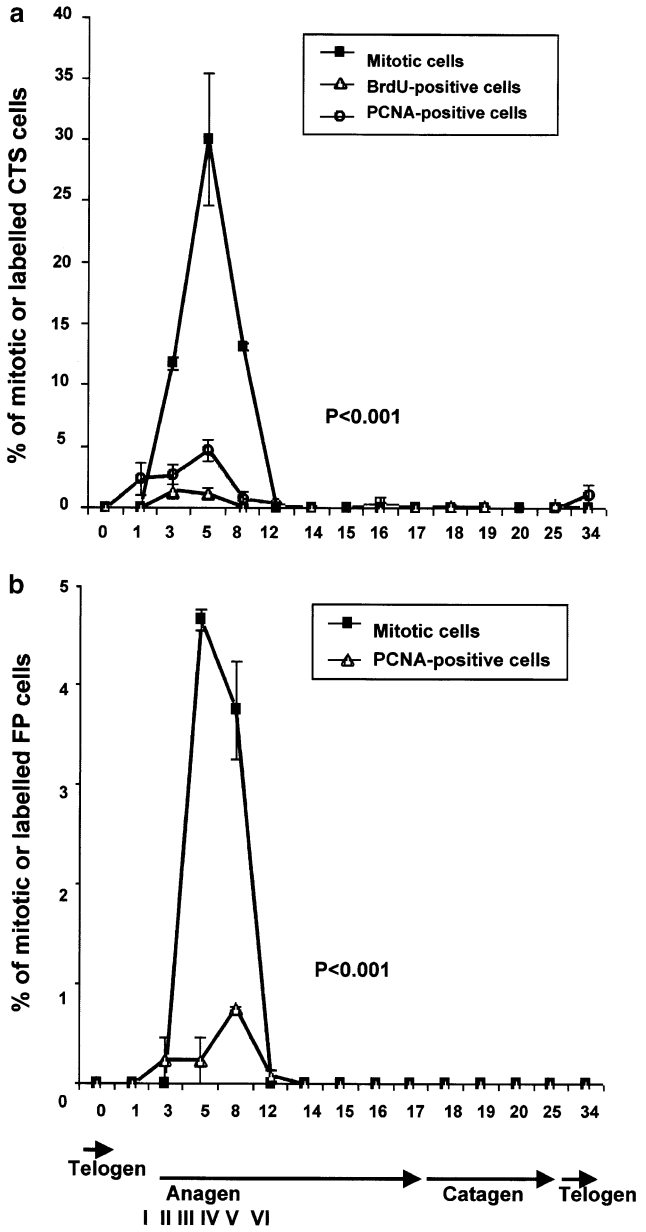

Figure 1. Histomorphometric analysis of the hair follicle mesenchyme during the hair growth cycle. (*a*) Cytokinetics of cells within the CTS during the telogen–anagen–catagen–telogen transitions. Note that CTS cell number increases from day 0, 2 days earlier than in the FP (see *b*). CTS proliferation reaches a maximum during anagen IV (i.e., day 5 postdepilation). (*b*) Cytokinetics of cells within the FP during the telogen–anagen–catagen–telogen transitions. Intra-FP cell proliferation does not occur until day 3 postdepilation (i.e., anagen II/III). Note also the different y-axis scales in (*a,b*).

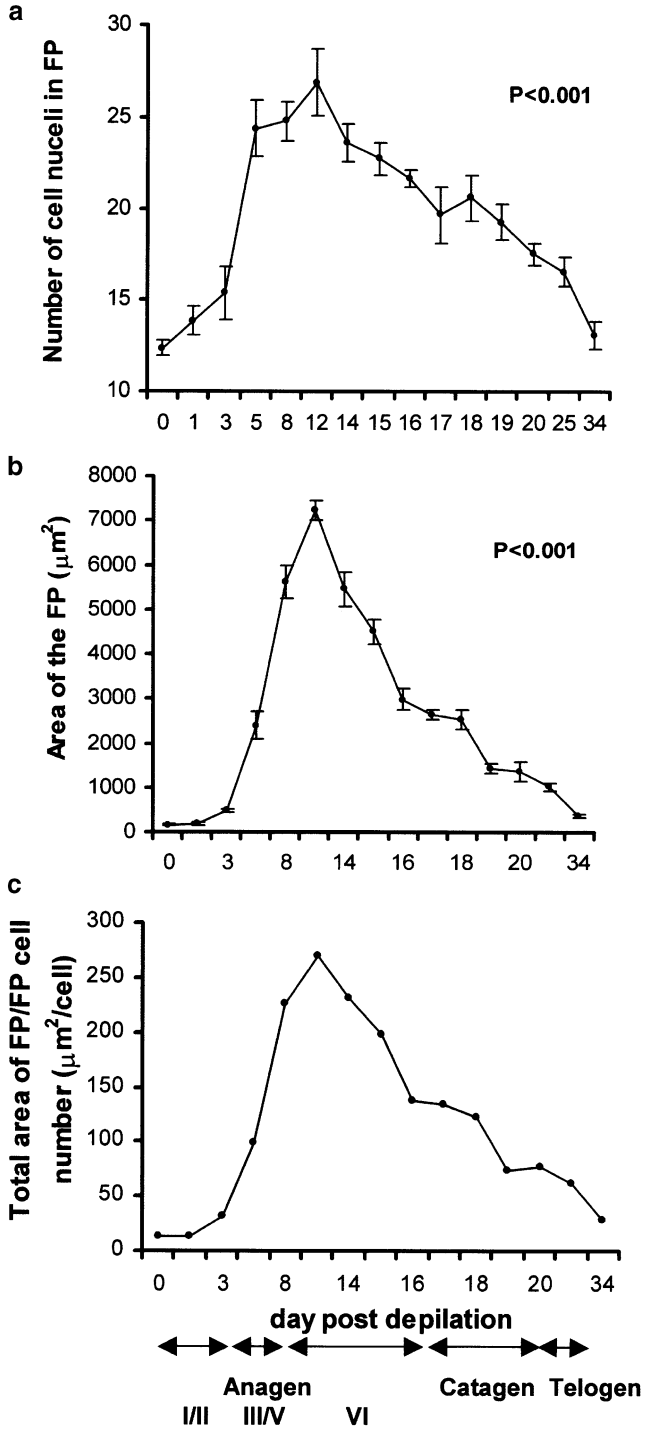

Figure 2. Planimetric analysis of the FP during the hair growth cycle. (*a*) Planimetric analysis of FP cell number during the telogen–anagen–catagen–telogen transitions. Cell number already increases at induction of anagen, i.e., day 0–1 and peaks at about day 12 (anagen VI). Note also the significant decline in FP cell numbers during most of anagen VI that continues further through to completion of catagen. (*b*) Planimetric analysis of total FP area (in μm^2) during the telogen–anagen–catagen–telogen transitions. FP size increases dramatically from day 3 to day 12 (i.e., anagen II/III to anagen VI) and thereafter rapidly declines. (*c*) Planimetric analysis of FP cell size/ECM volume (in μm^2) during the telogen–anagen–catagen telogen. This is an approximate measure of FP cell size and associated ECM volume. The size of FP cells and amount of ECM increases rapidly during anagen development and decreases again after the transition to full anagen is complete. Days postdepilation are indicated on the x-axis. Below this is a guide to hair cycle stage and component substages at different days of the depilation-induced murine hair cycle (Müller-Röver *et al*, 2001).

could not be measured directly, the ratio of total FP volume to the total cell number in the FP did provide an indirect measure of the combined FP cell and ECM volumes during the hair growth cycle. The 17-fold increase in this ratio from telogen to full anagen (**Fig 2*c***) concurred with the observation that FP cells were now distributed in copious ECM material. This was in marked contrast to the telogen-associated clustering of FP cells with their sparse ECM accompaniment (**Fig 4*d*** *vs* **Fig 5*f* and *g***). Increased metabolic and secretory activity was morphologically apparent in FP and in the more attenuated CTS-like cells during the telogen-to-anagen transition, as indicated by their increasing cytoplasmic volume and organelle content (**Fig 4*d***).

Reconstruction of the hair follicle epithelium correlates with spatial reorganization of the hair follicle mesenchyme during anagen development The mitotic index for both CTS and FP was highest during anagen IV (**Fig 1*a,b***), a substage of anagen characterized by the resumption of bulbar melanocyte proliferation and melanogenesis (**Fig 4*a,e,f***). Whereas the FP cell number at anagen IV was already 90% of maximal (**Fig 2*a***), the overall volume of the FP was only a third of maximum (**Fig 2*b***), reflecting both submaximal growth of both FP cells and their production of ECM (**Fig 2*c***). Importantly, the FP in anagen IV hair follicles is not yet fully invaginated by the developing hair follicle matrix and cells were still distributed randomly within the FP space (**Fig 4*a,e,f***). CTS cells within the FP were now most distinguishable, however, with the increasingly attenuated form of CTS cells contrasting with the round/oval FP cells (**Fig 4*a,d,f,g***). Nuclei of CTS cells additionally exhibited increased heterochromatism and basophilia (**Fig 4*a,d,f,g***).

The advance of anagen hair follicles to full anagen (i.e., anagen VI) was associated with a dramatic alteration in overall form of the FP (**Fig 4*g,h***). The almost complete invagination of the FP by the fully developed anagen VI hair matrix resulted in the FP assuming a greatly extended form whereby cells were most commonly distributed in single or double file (**Fig 4*g***). This reorganization of the FP space was associated with FP cells of pelage hair follicle switching their polarity from perpendicular (**Fig 4*d***) to parallel with the hair growth direction (**Fig 4*g,h***). Indeed, in some instances, contact between FP cell cytoplasmic processes and the matrix were observed (**Fig 4*i***). The FP and CTS were now more compartmentalized and morphologically distinct than at other times during the hair cycle, defined by the now complete development of the anagen hair follicle epithelium (**Fig 4*d,g***). The narrow channel of anagen VI FP cells was connected in the most proximal bulb to highly attenuated CTS fibroblasts (**Fig 4*g***). No cell proliferation was detected in CTS and FP just prior to or during full anagen (**Fig 1*a,b***). FP cells in full anagen exhibited high levels of cellular metabolism, as evidenced by their large cytoplasmic volumes, numerous mitochondria, very extensive endoplasmic reticulum, and Golgi apparatus.

The regression of the hair follicle mesenchyme during catagen involves FP cell emigration to the CTS, loss of synthetic activity, and cell death Cell proliferation was not observed in the FP and CTS of murine hair follicle during full anagen or during hair follicle regression (**Fig 1*a,b***). The anagen VI subphase continued from day 12 to 17 of the depilation-induced hair growth cycle (Müller-Röver *et al*, 2001). Unexpectedly, however, we found that the maximal size of the anagen VI FP was retained for only 1 d (i.e., day 12, **Fig 2*b***). By day 14, a full 25% reduction in total FP size was already observed (**Fig 2*b***). This reduction corresponded to a 13% decrease in FP cell number (**Fig 2*a***), with a further contribution from a reduction in ECM volume and FP cell size. By early catagen (day 17), the FP had lost a full two-thirds of its maximal anagen VI size (**Fig 2*b***), a third of its cells (**Fig 2*a***), and half of its cell size/ECM ratio (**Fig 2*c***). Further FP change during hair follicle regression (i.e., catagen I–VIII) was less marked (**Fig 1*a* and**

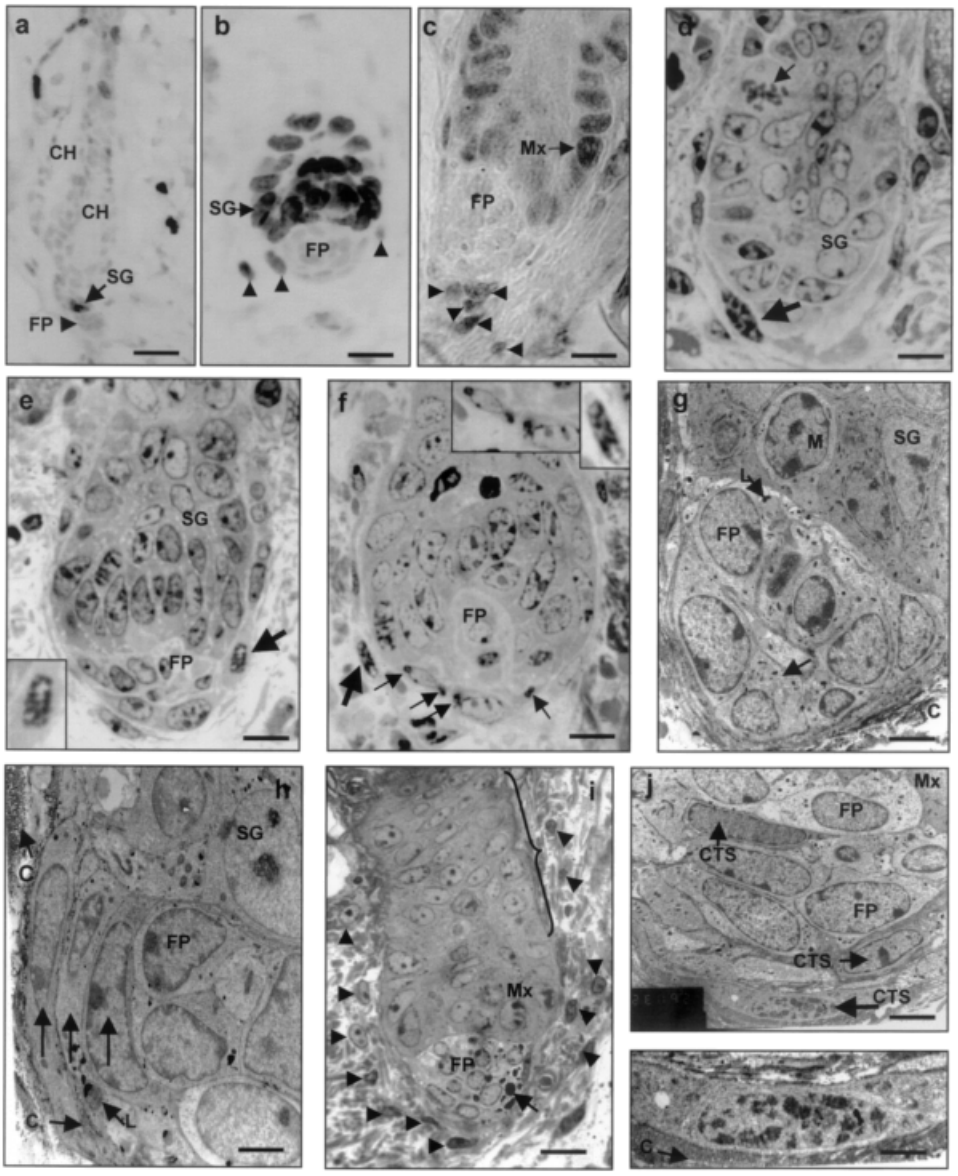

Figure 3. Morphologic and immunohistochemical analysis of the FP and CTS at onset of anagen. (*a*) Anagen I hair follicle at day 1 postdepilation. Ki67-positive cells are seen in the secondary germ (*arrow*) just above the FP (*arrowhead*). CH, club hair; SG, secondary germ. *Scale bar* = 20 μm. (*b*) Anagen II hair follicle at day 3 postdepilation. Ki67-positive cells are seen in the secondary germ (SG, *arrow*) and in the mesenchyme associated with the proximal CTS (*arrowheads*). Note that no Ki67-positive cells appear in the inner FP at this stage. *Scale bar* = 8 μm. (*c*) Anagen II/III hair follicle at day 3 postdepilation. PCNA-positive cells are seen in the developing hair matrix (Mx) and in the proximal CTS (*arrowheads*) close to the FP. Note the increasing numbers of cells in the FP but the absence of PCNA positivity inside the FP itself. *Scale bar* = 8 μm. (*d*) Spontaneous telogen to anagen transition at p28 (postpartum). Keratinocyte proliferation (*thin arrow*) begins in the SG. Note also that a CTS cell next to the hair follicle epithelium is undergoing mitosis (*thick arrow*). Toluidine blue. *Scale bar* = 7 μm. (*e*) Spontaneous anagen I at p28 (postpartum). Reorganization of the early anagen hair bulb. FP fibroblasts of variable morphologies and cytoplasmic volumes cluster beneath the reorganizing early-anagen hair bulb matrix. Note the presence of a proliferating fibroblast very close to the follicular papillary space (*arrowhead*). Inset: High magnification of proliferating cell. Toluidine blue. *Scale bar* = 7 μm. (*f*) Spontaneous anagen I at p28 (postpartum). Reorganization of the early anagen hair bulb including invagination of the early FP. Note the presence of two fibroblasts containing melanin from the previous pigmented bulb (*thin arrows*). These cells are located immediately outside the developing FP and are positioned next to a proliferating CTS cell (*thick arrow*). Inset: High magnification of melanin-containing cells and proliferating cell. Toluidine blue. *Scale bar* = 7 μm. (*g*) Telogen/anagen I hair follicle at day 0 postdepilation. The FP exists as a small number of tightly clustered heterogeneous cells. Note that some FP cells exhibit increased nuclear euchromatism and cytoplasmic volume with greater organelle density (*arrow*). Telogen-associated lipid droplets remain in some cells (L). An inactive melanocyte (M) is located in the SG in contact with the basal lamina separating the epithelium and mesenchyme. C, collagen. Uranyl acetate and lead citrate. *Scale bar* = 4 μm. (*h*) Anagen I hair follicle, day 1 postdepilation. The FP exists as a tight ball of heterogeneous cells. Note the cells at the periphery of the FP exhibit extended CTS cell-like morphologies (*arrows*). Some of the CTS-like cells are in direct physical contact with more typical FP cells (FP), whereas others are located both inside and outside collagen bundles (C). Telogen-associated lipid droplets (L) remain within some FP cells. C, collagen. Uranyl acetate and lead citrate. *Scale bar* = 3 μm. (*i*) Anagen I/II hair follicle, day 3 postdepilation. The developing matrix (Mx) grows around the still-clustered ball of FP cells. Melanin granules (*arrow*) from the previous melanogenic phase are located within FP cells. Note that many mesenchymal cells are distributed close, but not attached to the CTS at this stage (*arrowheads*). Few cells are directly associated with the CTS itself ({}). Toluidine blue. *Scale bar* = 8 μm. (*j*) Anagen I hair follicle, day 1 postdepilation. FP cells are now distributed more randomly than during telogen. Cells exhibit increased nuclear euchromatism, cytoplasmic density and volume, and organelle content. Note the close interaction between typical FP cells and cells with typical CTS cell morphology. These latter cells are not restricted to the periphery of the FP but are now found "within" the FP. Note the typical CTS cell in early mitosis (M). Mx, matrix; C, collagen. (Inset: high power view of mitotic CTS fibroblast.) Uranyl acetate and lead citrate. *Scale bar* = 4 μm. Inset: 2 μm.

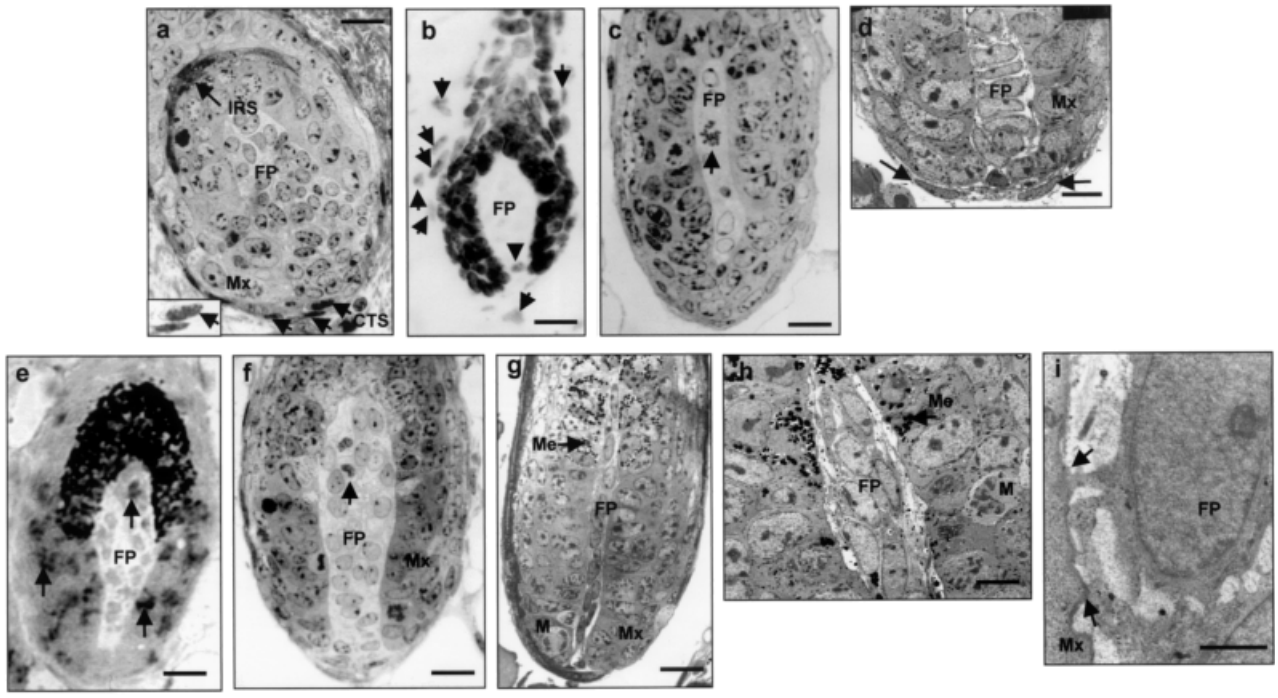

Figure 4. Morphologic and immunohistochemical analysis of the FP and CTS during mid to late anagen development. (*a*) Anagen III/IV hair follicle, day 3 postdepilation. FP cells are now more numerous and are distributed more randomly than during telogen. Cells contain oval nuclei with increased euchromatism and exhibit increased cytoplasmic volume. A mitotic fibroblast is seen in the proximal CTS at the base of the FP (*arrow* and inset). CTS cells exhibit increasingly attenuated and heterochromatic forms (*arrows*). Mx, matrix; IRS, inner root sheath. Toluidine blue. *Scale bar* = 10 μm. (*b*) Anagen III/IV hair follicle, day 3 postdepilation. Several Ki67-positive cells are observed in the CTS (*arrows*) and also within the FP itself (*arrowhead*). *Scale bar* = 12 μm. (*c*) Spontaneous anagen III at p28 (postpartum day 28). This oblique section exhibits the early anagen hair follicle where much of the FP is within the hair bulb matrix. Note that one of the FP fibroblasts is in mitosis (*arrow*). Toluidine blue. *Scale bar* = 7 μm. (*d*) Anagen IV hair follicle, day 2 postdepilation. FP cells are now more numerous and distributed in a highly organized manner with the cell's long axis perpendicular to the hair growth direction. FP cells display active cytoplasm with high organelle content. Note the highly extended and electron-dense appearance of CTS (*arrow*) cells located "outside" the FP space. Mx, matrix. Uranyl acetate and lead citrate. *Scale bar* = 6 μm. (*e*) Anagen VI hair follicle. Ki67-positive cell is located within the FP proper (*arrow*) and in the matrix (Mx) epithelium. *Scale bar* = 12 μm. (*f*) Spontaneous anagen IV at p28 (postpartum). This longitudinal section exhibits an early anagen hair bulb with recently activated melanogenesis. Note that one of the FP fibroblasts has just completed mitosis, and now exists as two daughter cells (*arrow*). Toluidine blue. *Scale bar* = 7 μm. (*g*) Anagen VI hair follicle, day 12 postdepilation. FP cells are now distributed parallel to the growth axis and extend deep into the hair matrix (Mx) where they reach a maximal surface area interface with the proliferating matrix (Mx). Me, melanin. Uranyl acetate and lead citrate. *Scale bar* = 6 μm. (*h*) Anagen VI hair follicle, day 12 postdepilation. FP cells are oriented parallel to the growth axis and contain melanin granules (Me). Note also the increase intracellular space that is filled with ECM and isolated melanin granules transferred from adjacent matrix (Mx). M, mitotic keratinocyte. Toluidine blue. *Scale bar* = 10 μm. (*i*) Anagen VI hair follicle, day 12 postdepilation. FP cells form heterotypic contacts (*arrows*) with the adjacent matrix via cytoplasmic process that perforate the basal lamina separating matrix epithelium from FP mesenchyme (*arrow*). Uranyl acetate and lead citrate. *Scale bar* = 1 μm.

2*a–c*); however, despite the only slight further reduction in FP cell numbers during the progression of hair follicle regression, catagen was associated with a ≈45% reduction in both overall FP size and FP cell size/ECM ratio (**Fig 2*a,c***).

The literature is remarkably silent on the fate of the CTS and FP cell subpopulations during hair follicle regression. It is reasonable to expect, however, that in any self-renewing system such as the hair follicle, significant cell proliferation during stages of growth should be balanced by cell deletion during regression. This was indeed appreciated for the regressing hair follicle epithelium, which exhibited high levels of keratinocyte apoptosis during catagen (**Fig 5*a–d***) (Weedon and Strutton, 1981; Lindner *et al*, 1997). In line with the complete absence of TUNEL-positive cells in the FP during catagen (Lindner *et al*, 1997), morphologic/ultrastructural signs of apoptosis were undetectable in the FP at any stage of the hair cycle. Therefore, the possibility of FP cell emigration to the CTS was considered. Surprisingly, increased cellularity was not evident in the later stages of anagen VI/catagen CTS. Instead, occasional apoptotic bodies were found in the CTS itself (**Fig 5*b–e***). The mesenchymal nature of these cells undergoing apoptosis was indicated by their distribution within a collagenrich environment, the absence of ultrastructural epithelial cell markers and their lack of association with collapsing perifollicular microvasculature.

By high-resolution light microscopic analysis we tracked the fate of CTS cells in the regressing hair follicle. We found that some CTS fibroblasts lost their anagen-associated attenuated form, due in part to increased nuclear to cytoplasmic ratio, with CTS cell nuclei adopting highly indented forms (**Fig 5*a***). Notably, CTS cells appeared to be "lost" from the regressing hair follicle. This seemed to occur via their "detachment" from the increasingly corrugated glassy membrane. Indeed, much of the resorbing glassy membrane, which appeared acellular at this stage, was associated instead with clear-staining macrophages (**Fig 5*a,c,d***). FP cell nuclei also became pleomorphic, heterochromatic, and indented (**Fig 5*b***).

The "quiescent" hair follicle mesenchyme during telogen shows evidence of residual activity The total number of cells within the telogen FP was significantly reduced to approximately 12 cells/HF from a high of 27 cells/HF in full anagen (**Fig 2*a***). Planimetric analysis of telogen FP further revealed that this reduction in cell number accounted for only part of an over 40-fold reduction in overall FP size (**Fig 2*b***). Much of the observed reduction in total FP size, i.e., from 7200

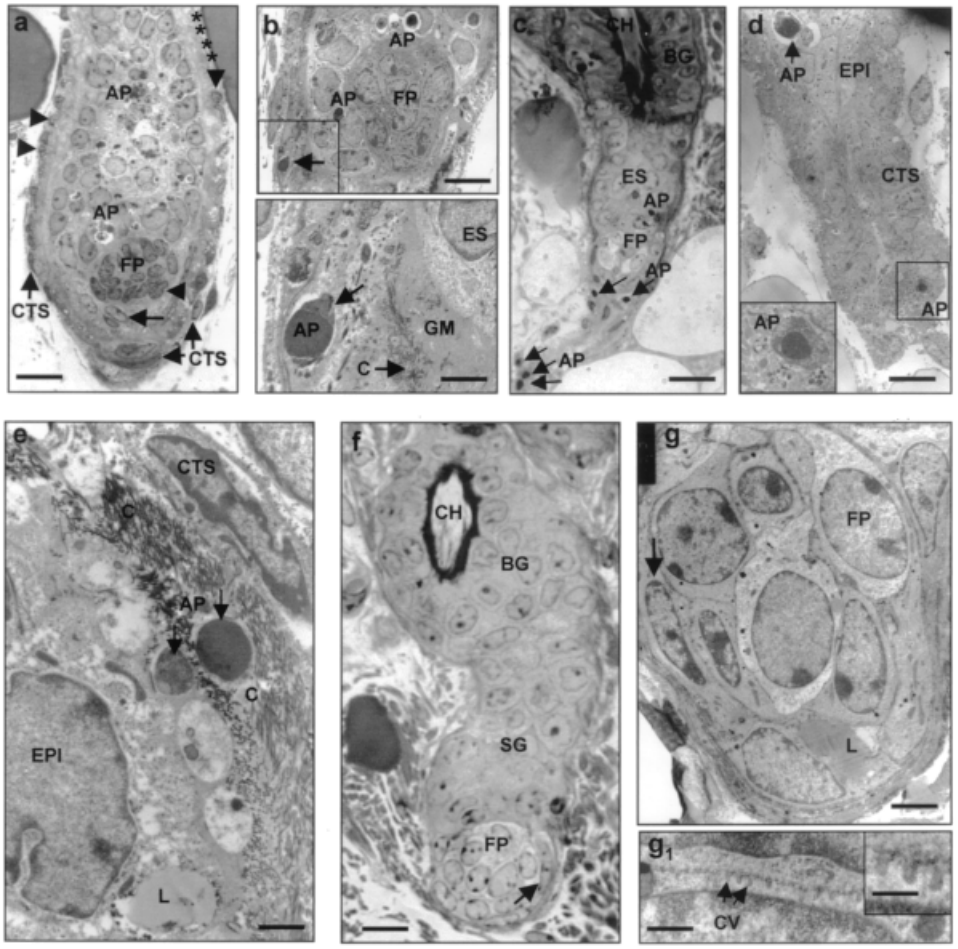

Figure 5. Morphologic and immunohistochemical analysis of the FP and CTS during hair follicle regression (catagen). (*a*) Catagen V/VI hair follicle, day 19 postdepilation. FP cells have resumed their telogen-like clustered form. Cells contain heterochromatic nuclei with pleomorphic forms (*arrowhead*). CTS-like cells with extended morphologies are seen close by (*arrow*) midway between the FP cluster and the peripheral CTS population (CTS). The distribution of cells within the CTS is uneven with several regions of the CTS appearing acellular (*). Remaining CTS cells exhibit increased nuclear pleomorphism (*arrowhead*). AP; keratinocyte apoptosis. Toluidine blue. *Scale bar* = 8 μm. (*b*) Catagen VI hair follicle, day 19 postdepilation. Apoptotic keratinocytes (AP) surround a cluster of FP cells that exhibit heterochromatic and pleomorphic nuclei. Apoptosis in the CTS (*arrow*). Inset: High-power view of apoptotic cells in the CTS. C, Collagen. Uranyl acetate and lead citrate. *Scale bar* = 6 μm. Inset = 1.5 μm. (*c*) Catagen VII hair follicle, day 19 postdepilation. Apoptotic keratinocytes (AP) surround a small cluster of heterogeneous FP cells. Note that the trailing CTS containing several apoptotic cells (AP). Toluidine blue. *Scale bar* = 8 μm. (*d*) Catagen VII hair follicle, day 19 postdepilation. High-power view of apoptotic cells (AP) in the epithelial strand (EPI) and trailing CTS. Inset: High-power view of cell in early stage of apoptosis. Uranyl acetate and lead citrate. *Scale bar* = 7 μm. (*e*) Catagen VII hair follicle, day 19 postdepilation. Note the apoptotic bodies in the CTS (AP) surrounded by collagen bundles (c). These cells are clearly located outside the hair follicle epithelium (EPI). L, lipid droplets. Uranyl acetate and lead citrate. *Scale bar* = 1.5 μm. (*f*) Telogen hair follicle (obliquely cut). The FP consists of a tight ball of cells that exhibit a high nuclear to cytoplasmic ratio. Note the very close association between FP cells and the more extended CTS fibroblasts (*arrow*). "Bulge" stem cells with cerebriform nuclei (BG); SG, secondary germ; CH, club hair. Toluidine blue. *Scale bar* = 8 μm. (*g*) Telogen FP. The FP consists of a tight ball of heterogeneous cells. Cells vary in level of nuclear heterochromatism, cytoplasmic density and volume, and nuclear to cytoplasmic ratio. Note the close association between FP cells and the more extended CTS fibroblasts (*arrow*). Some FP cells contain lipid droplets (L). Inset: High-power view of FP cell membranes showing numerous caveolae (CV). Uranyl acetate and lead citrate. *Scale bar* = 3 μm. g_1 = 1 μm. Inset: 0.4 μm.

μm^2 in full anagen to 164 μm^2 in telogen, was due a 20-fold reduction in FP cell size/ECM volume ratio (**Fig 2*c***). The FP during telogen formed a heterogeneous ball of fewer, mostly rounded, cells with high nuclear to cytoplasmic ratios and moderately heterochromatic nuclei (**Fig 5*f,g***). These features reflected an overall low level of cellular activity in these cells. Although mesenchymal cells that remained within the telogen FP displayed many features of cellular quiescence, including formation of lipid droplets (**Fig 5*g***), these cells were now distributed in closer apposition to each other than at any other phase of the hair follicle growth cycle (**Fig 5*f,g***). Furthermore, although still separated by a thin basal lamina (**Fig 5*g***), these cells also were in close contact with epithelial cells of the secondary germ. Both types of close physical associations were facilitated primarily by the dramatic reduction in ECM during catagen (**Fig 2*c***). Telogen was also associated with the loss of a clear morphologic distinction between FP and CTS cells, although FP cells retain close contact with more attenuated CTS-like cells located at the FP periphery (**Fig 5*f***). Upon close ultrastructural examination, intercellular plasma membrane specializations including numerous caveolae were observed in telogen FP cells (**Fig 5*g*, inset**). These omega-shaped plasma membrane in-foldings were asymmetrically distributed, i.e., were commonly located on one of two adjacent cell membranes of the FP cells in telogen hair follicles.

DISCUSSION

Much of the mystery surrounding mesenchymal cell dynamics during the hair growth cycle derives from the prevailing belief that the CTS and FP represent very stable populations of

fibroblasts (Wessells and Roessner, 1965; Pierard and de la Brassinne, 1975; Tezuka *et al*, 1991). Our study yielded the rather unexpected finding that the reconstructing hair follicle mesenchyme contains many fibroblasts that proliferate actively in the CTS during the earliest stages of anagen (**Fig 6**, anagen I) and that they do so before any proliferation is detectable within the FP. The significant increase in total FP cell number before the occurrence of intrapapillary fibroblast proliferation, strongly suggests that the CTS is the likely source of a significant number of anagen FP cells and that the migration of cells from the mitotically-active CTS into the FP is responsible for much of the 2-fold increase in FP cells during anagen development (**Fig 6**, anagen II and III/IV). Moreover, their contrasting peak mitotic indices (30% *vs* 5%) also strongly indicates that it is the CTS that drives the cytokinetic changes in the early anagen FP. Further support for this view derives from ultrastructural and immunohistochemical evidence of proliferating CTS-like fibroblasts located around the periphery of the early anagen FP.

Therefore, the HF mesenchyme displays much greater plasticity and cytokinetic dynamics than previously appreciated, including intense and stringently controlled, bidirectional, hair cycle-dependent fibroblast trafficking between the FP and the CTS, with cell proliferation in the CTS likely serving as the driving force behind reconstruction of the anagen FP.

The anagen-associated migration of CTS fibroblasts into the FP is complemented by a later, minor proliferative activity within the FP itself. An additional contributing factor to the growing size of the FP during anagen is increased FP cell size and an increased synthesis and secretion of ECM. The developing hair follicle epithelium that grows around the FP remodels the spatial organization of FP cells within the hair follicle. Thereafter, FP cell number and size remain maximal for a short period during full anagen and thereafter, rapidly decrease via cell emigration from the FP to the CTS, followed by limited localized fibroblast apoptosis in the regressing CTS during catagen.

This study unequivocally demonstrates that fibroblasts of the proximal CTS proliferate throughout anagen I–VI, yet with substantial hair cycle stage-specific differences in their level of proliferative activity (**Fig 1*a***). In addition, we show that fibroblasts within the FP itself divide, albeit at a low level and only during a restricted period of hair follicle cycling (i.e., anagen III–anagen V) (**Fig 4**). Both findings compel one to reject the conventional wisdom that views the hair follicle mesenchyme as a stable mesenchymal cell population without proliferative potential (Wessells and Roessner, 1965; Pierard and de la Brassinne, 1975; Tezuka *et al*, 1991). The brevity of the period during which FP proliferation is detectable and the very low level of proliferative activity in the FP may have invited this misconception. Both spontaneous and depilation-induced murine hair follicle cycling were studied, as this not only allows to study a capillary-free FP (Durward and Rudall, 1958) so as to avoid ambiguities affecting data interpretation of proliferating cells in the vascularized human FP, but also as this increases the chance of detecting limited, time-restricted mesenchymal proliferation. As fibroblast proliferative activity was detected both in depilation-induced and spontaneous early anagen (**Fig 3*b–f***), the former does not add significant artifactual cell migration in early anagen, justifying the further use of this optimally synchronized hair follicle cycling model for dissecting mesenchymal dynamics.

One must be careful not to overinterpret the proliferative potential of FP cells, as it is altogether possible that proliferation in this hair follicle mesenchyme component extends only to recent migrants from the proliferatively active CTS (**Fig 6**, anagen III/IV and V). This would explain the strikingly different mitotic indices of CTS and FP, and is also supported by the morphologically heterogeneous intra-FP cell populations at this stage (**Fig 3*h–j***). It is of note here that previous *in vitro* work has shown movement of CTS cells into the FP space in long-term hair follicle organ cultures (Jahoda, 1998). These data provide a mechanism to explain the regeneration of a FP from the lower CTS after wounding (Reynolds *et al*, 1999; Jahoda and Reynolds, 2001) and suggest the hypothesis that the terminal-to-vellus transformation of hair follicles during androgenetic alopecia may, at least in part, be due to emigration of fibroblasts from the FP to the CTS (Whiting, 2001). Together these findings strongly suggest that the CTS is the major driver of the reconstruction of the anagen FP and so may indirectly orchestrate the composition of the anagen-inductive microenvironment of the FP. The CTS is more accessible than the FP, and should be viewed as a major target for pharmacologic intervention in hair growth studies. It is of interest, therefore, to note the significant ^{3}H-thymidine incorporation in the CTS and FP of hair follicle of minoxidil-treated scalp skin of stump-tailed macaques (Uno *et al*, 1987).

The exact source of CTS progenitor cells in the developing anagen hair follicle is still unclear. Possible sources may include residual cells attached to the periphery of the telogen club or mesenchymal cells in the neighboring dermis. Some clues may be deduced from our finding that, as the new hair follicle lengthens, "free" mesenchymal cells associate with the proximal margins of the growing hair follicle (**Fig 6**, anagen I). These cells may represent pre-CTS fibroblasts and/or a hair follicle mesenchyme reservoir, as they do appear to be more than casually associated with the regrowing hair follicle as they locate close to acellular regions of the mid and distal regions of the early anagen CTS. The regeneration of a functional FP from CTS (Reynolds *et al*, 1999) proves that this sheath can act to provide a fully functional FP cell reservoir.

Whereas the CTS may drive the early stages of anagen development by repopulating the FP, doubling of FP cell number accounts for only a part of the 14-fold increase in overall size of the FP during early anagen (**Fig 2*b***). We need to consider the combined contribution of increased FP cell size and increased production of ECM by the anagen FP (Van Scott and Ekel, 1958; Elliott *et al*, 1999). Increased cell size and activity were appreciated ultrastructurally via increased cytoplasmic/nuclear ratios and the associated increase in organelles involved in metabolism, e.g., mitochondria, endoplasmic reticulum, Golgi complex, and increased production of ECM proteins (Jahoda, 1998).

Any discussion of mesenchymal–epithelial interactions in organogenesis also requires full consideration of epithelial influences on the mesenchyme. One example of this that is addressed in the current study is the dramatic re-orientation of FP cells from perpendicular to parallel to hair growth direction as the hair cycle progresses from anagen IV to full anagen VI in murine pelage hair follicles. The change from a random cell distribution to a highly organized and highly extended channel of cells bounded on all sides by the maturing hair matrix (**Fig 6**), is likely to extend FP-derived effects, e.g., morphogens/mitogens, to the greatest number of both germinative and differentiating hair follicle matrix cells (Link *et al*, 1990; Jahoda and Reynolds, 1996). It is notable, therefore, that the mitotic indices for both CTS and FP cells decline dramatically upon transition to anagen IV—when there is a major upregulation of differentiation complexity (Langbein *et al*, 2001; Stenn and Paus, 2001). No further proliferation occurs in the FP or the CTS during the middle and late stages of anagen VI (**Fig 1*a***), a period of maximal hair shaft production.

A rather unexpected finding of this study, however, was the observation that FP cell number actually decreases within 1–2 d of reaching anagen VI (i.e., during early anagen VI). Indeed, by the time the hair follicle was only a third way through full anagen, a full 25% of FP cells are lost (**Fig 2*a***). One possible interpretation of this finding is that a full complement of FP cells is needed only at the start of anagen VI, perhaps when morphogen demands by the highly proliferative and subsequently differentiating matrix keratinocytes are at their greatest. Interestingly, this reduction in FP cell number does not appear to cause any change of hair shaft caliber. This cautions against the—perhaps overly simplistic—dogma of strict FP/matrix volume proportionality (Van Scott and Ekel, 1958), and suggests that more complex epithelial–mesenchymal interactions determine the FP/matrix ratio.

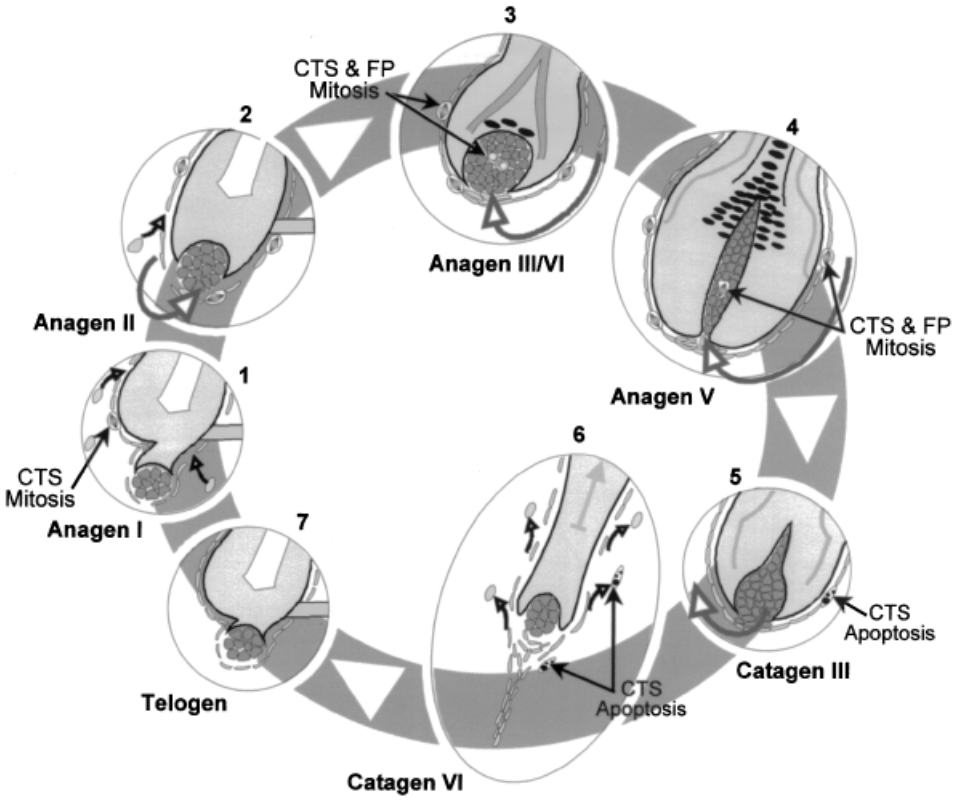

Figure 6. Schematic of proposed mesenchymal cell dynamics during murine hair growth cycle. (1) Anagen I: Specialized fibroblasts from the near dermis and/or permanent portion of the CTS attach to the reconstructing CTS (see **Fig 3*b***). Cell proliferation occurs in the CTS (see **Fig 3*b–f***). (2) Anagen II: Increased CTS proliferation. Note increasing cell number in FP and expansion of epithelial matrix around upper FP (see **Figs 1*a,b,* 2*a***). (3) Anagen III/IV: Cell proliferation continues in CTS and is now occasionally also seen in FP. Note dramatic increase in FP cell number and commencement of inner root sheath production and hair follicle melanogenesis (see **Figs 1*a,b,* 4*a–c,e,f***). (4) Anagen V: Cell proliferation continues in CTS and rarely in FP (see **Figs 1*a,* 4*e,f***). FP cells reorganize into an extending channel of cells that exhibit increased reciprocal surface area with hair bulb matrix keratinocytes (see **Fig 4*g,h***). (5) Catagen III: Significant loss of FP cells occurs before end of anagen VI (see **Fig 2*a***) and continues during catagen. Cells appear to migrate out of FP and into CTS (see **Fig 5*a,b***). Apoptosis occurs in CTS but not in FP (see **Fig 5*b***). (6) Catagen VI: FP cells continue to migrate into CTS (see **Fig 5*c,d***). Some cells detach from CTS scaffold and some undergo apoptosis (see **Fig 5*c–e***). (7) Telogen: A reduced complement of FP fibroblasts remain during telogen as a discrete ball of tightly linked cells (see **Fig 5*f,g***). Few fibroblasts may be seen in the periphery of the telogen papilla.

Whereas apoptosis drives the regression of the lower hair follicle epithelium during catagen (Lindner *et al*, 1997), the events that underlie regression of the hair follicle mesenchyme are much less clear (Westgate *et al*, 1991; Jahoda *et al*, 1992). It is reasonable to suppose that in any self-renewing system such as the hair follicle, significant cell proliferation during stages of growth are balanced by cell "loss" during regression. It is rather remarkable, therefore, that apoptosis is not detectable in the FP at any hair cycle stage, perhaps due to high expression levels of the anti-apoptotic factor bcl-2 (Lindner *et al*, 1997; Jahoda, 1998; Tobin *et al*, 1998). This conundrum appears to be explained by an efflux of FP cells into the proximal CTS and/or dermis (**Figs 5 and 6**).

Despite this exodus, up to 50% of FP cells do remain in place (**Fig 2*a***), suggesting that only a partial replacement of FP cells is necessary during the changeover between two successive hair cycles. Morphologic data provide some support for this view: catagen FP cells assume an increasing heterogeneity that may reveal some division of labor; e.g., melanin-accepting fibroblasts, ciliated fibroblasts, etc., suggestive of the existence of different FP cell subpopulations. FP cell emigration to CTS could be expected to increase total CTS cell numbers, at least towards the end of anagen VI. Surprisingly, however, no increase in the cellularity of the CTS was apparent morphologically (**Fig 5*a***). This second conundrum may be resolved by the rare examples of apoptosis that occur within the CTS proper (**Figs 5 and 6**). These apoptotic cells may indeed be deleted émigrés from the FP, CTS cells themselves, or other connective tissue cells, e.g., mast cells or endothelium. Irrespective of their true identity, one might expect that these cells would not share the apoptosis protection apparently conferred by bcl-2 in the FP. It is notable, therefore, that, whereas high expression of bcl-2 by the FP is maintained throughout the hair growth cycle, the CTS is relatively bcl-2-negative during catagen and telogen (Stenn *et al*, 1994; Lindner *et al*, 1997).

We know very little about the true nature of the fibroblasts that remain in the telogen FP. It is easy to see why the telogen FP has been termed "resting", presumably due to the lack of a need to support further the regressed hair follicle epithelium. The hair follicle, however, does not appear to be fully switched off during telogen. Not only are telogen FP cells distributed more closely to each other than at any other stage of the hair cycle, intimate cell–cell contacts are evident via cell membrane specializations. Prominent among these were the flask-like infoldings of the plasma membrane commonly termed caveolae, which in other tissues are associated with active endocytosis and exocytosis and are implicated in intercellular signal transduction (Fielding, 2001). Moreover, the increasing cell heterogeneity of FP cells seen during catagen and telogen is suggestive of distinct FP cell subpopulations that may be associated with a significant division of labor in this hair follicle mesenchymal component.

While not directly examined in this study, our results also have important implications for the study of the mechanisms that underlie clinically important hair follicle transformations (Jahoda, 1998; Whiting, 2001). These include vellus-to-terminal transformations associated with hair growth during puberty, hirsuitism,

and hypertrichosis (Deplewski and Rosenfield, 2000). Similarly, it is likely that modulation of hair follicle mesenchymal dynamics accounts for terminal-to-vellus transformations in androgenetic alopecia (Barth, 1987; Ishino *et al*, 1997; Whiting, 2001). Such events may result from the modulation of FP cell migration to a less apoptosis-resistant CTS throughout anagen VI to telogen (and vice-versa during early anagen), and may be under the local control of regulatory molecules such as androgens. In this way, the rapid changes in hair fiber volume seen during puberty may be facilitated within a single hair cycle, much like it has been postulated to occur during androgenetic alopecia when rapid hair follicle miniaturization probably can be executed even within a single hair growth cycle (Whiting, 2001).

In summary, the plasticity of the FP and CTS and the bidirectional trafficking of the fibroblasts in these mesenchymal components of the hair follicle are likely to be a critical element for hair cycle control. In addition, the hair follicle offers us a very instructive model for studying mesenchymal dynamics of specialized fibroblasts with morphogenic properties in general. To exploit the full potential of these hair follicle mesenchymal cell subpopulations, we also will need to understand more fully the controls of fibroblast death, migration, and secretory behavior within the hair follicle mesenchyme. This will have important clinical implications for any alterations in FP cell number that lie at the heart of clinically observed increases and decreases in hair fiber size, such as in hirsutism and androgenetic alopecia.

This study was supported in part by grants to RP from Deutsche Forchunggemeinschaft (DFG, Pa 345/8–3) and Cutech Srl., Italy; to AG from the Russian Fund for Basic Research (00–04–48043) and from President of Russian Federation for Young Doctors in Science (00–15–99365) and to DJT from the Department of Biomedical Sciences, University of Bradford.

REFERENCES

Adelson DL, Kelley BA: Increase in dermal papilla cells by proliferation during development of the primary wool follicle. *Aust J Agric Res* 43:843–856, 1992

Barth JH: Normal hair growth in children. *Pediatr Dermatol* 4:173–184, 1987

Cohen J: Transplantation of individual rat and guinea pig whisker papilla. *J Embryol Exp Morph* 9:117–127, 1961

Cotsarelis G, Millar SE: Towards a molecular understanding of hair loss and its treatment. *Trends Mol Med* 7:293–301, 2001

Deplewski D, Rosenfield RL: Role of hormones in pilosebaceous unit development. *Endocr Rev* 21:363–392, 2000

Durward A, Rudall KM: The vascularity and patterns of growth of hair follicles. In: Montagna W, Ellis RA (eds). *The Biology of Hair Growth.* New York: Academic Press, 1958; p 469–485

Elliott K, Stephenson TJ, Messenger AG: Differences in hair follicle dermal papilla volume are due to ECM volume and cell number: Implications for the control of hair follicle size and androgen responses. *J Invest Dermatol* 113:873–877, 1999

Fielding CJ: Caveolae and signaling. *Curr Opin Lipidol* 12:281–287, 2001

Horne KA, Jahoda CA: Restoration of hair growth by surgical implantation of follicular dermal sheath. *Development* 116:563–571, 1992

Hutchinson PE, Thompson JR: The cross-sectional size and shape of human terminal scalp hair. *Br J Dermatol* 136:159–165, 1997

Ibrahim L, Wright EA: A quantitative study of hair growth using mouse and rat vibrissal follicles. I. Dermal papilla volume determines hair volume. *J Embryol Exp Morph* 72:209–222, 1982

Ishino A, Uzuka M, Tsuji Y, Nakanishi J, Hanzawa N, Imamura S: Progressive decrease in hair diameter in Japanese with male pattern baldness. *J Dermatol* 24:758–764, 1997

Jahoda CA: Cellular and developmental aspects of androgenetic alopecia. *Exp Dermatol* 7:235–248, 1998

Jahoda CA, Reynolds AJ: Dermal–epidermal interactions. Adult follicle-derived cell populations and hair growth. *Dermatol Clin* 4:573–583, 1996

Jahoda CA, Reynolds AJ: Hair follicle dermal sheath cells: Unsung participants in wound healing. *Lancet* 358:1445–1448, 2001

Jahoda CA, Horne KA, Oliver RF: Induction of hair growth by implantation of cultured dermal papilla cells. *Nature* 311:560–562, 1984

Jahoda CA, Reynolds AJ, Chaponnier C, Forester JC, Gabbiani G: Smooth muscle alpha-actin is a marker for hair follicle dermis *in vivo* and *in vitro*. *J Cell Sci* 99:627–636, 1991

Jahoda CA, Mauger A, Bard S, Sengel P: Changes in fibronectin, laminin and type IV collagen distribution relate to basement membrane restructuring during the rat vibrissa follicle hair growth cycle. *J Anat* 181:47–60, 1992

Kishimoto J, Burgeson RE, Morgan BA: Wnt signaling maintains the hair-inducing activity of the dermal papilla. *Genes Dev* 14:1181–1185, 2000

Langbein L, Rogers MA, Winter H, Praetzel S, Schweizer J: The catalog of human hair keratins. II. Expression of the six type II members in the hair follicle and the combined catalog of human type I and II keratins. *J Biol Chem* 276:35123–35132, 2001

Lindner G, Botchkarev VA, Botchkareva NV, Ling G, van der Veen C, Paus R: Analysis of apoptosis during hair follicle regression (catagen). *Am J Pathol* 151:1601–1617, 1997

Lindner G, Menrad A, Gherardi E, *et al*: Involvement of hepatocyte growth factor/scatter factor and met receptor signaling in hair follicle morphogenesis and cycling. *FASEB J* 14:319–332, 2000

Link RE, Paus R, Stenn KS, Kuklinska E, Moellmann G: Epithelial growth by rat vibrissae follicles *in vitro* requires mesenchymal contact via native ECM. *J Invest Dermatol* 95:202–207, 1990

Magerl M, Tobin DJ, Müller-Röver S, Hagen E, Lindner G, McKay I, Paus R: Patterns of proliferation and apoptosis during murine hair follicle morphogenesis. *J Invest Dermatol* 116:947–955, 2001

Matsuzaki T, Inamatsu M, Yoshizato K: The upper dermal sheath has a potential to regenerate the hair in the rat follicular epidermis. *Differentiation* 60:287–297, 1996

Matsuzaki T, Yoshizato K: Role of hair papilla cells on induction and regeneration processes of hair follicles. *Wound Repair Regen* 6:524–530, 1998

Montagna W, Parakkal PF: *The Structure and Function of Skin.* New York: Academic Press, 1974

Müller-Röver S, Handjiski B, van der Veen C, Eichmuller S, Foitzik K, McKay IA, Stenn KS, Paus R: A comprehensive guide for the accurate classification of murine hair follicles in district hair cycle stages. *J Invest Dermatol* 117:3–15, 2001

Oliver RF: The experimental induction of whisker growth in the hooded rat by implantation of dermal papillae. *J Embryol Exp Morph* 18:43–51, 1967

Parakkal PF: Catagen and telogen phases of the growth cycle. In: Orfanos CE, Happle R (eds). *Hair and Hair Diseases.* Berlin: Springer-Verlag, 1990; p 99–116

Panteleyev AA, Paus R, Ahmad W, Sundberg JP, Christiano AM: Molecular and functional aspects of the hairless (hr) gene in laboratory rodents and humans. *Exp Dermatol* 7:249–267, 1998

Paus R, Cotsarelis G: The biology of hair follicles. *N Engl J Med* 341:491–497, 1999

Paus R, Stenn KS, Link RE: Telogen skin contains an inhibitor of hair growth. *Br J Dermatol* 122:777–784, 1990

Paus R, Müller-Röver S, Botchkarev VA: Chronobiology of the hair follicle: Hunting the "hair cycle clock". *J Invest Dermatol Symp Proc* 4:338–345, 1999

Philpott MJ, Paus R: Principles of hair follicle morphogenesis. *Molecular Basis of Epithelial Appendage Morphogenesis*. Chuong C-M (eds). Austin, Texas: R.G. Landes Company, 1998; p 75–103

Pierard GE, de la Brassinne M: Modulation of dermal cell activity during hair growth in the rat. *J Cutan Pathol* 35–41, 1975

Reynolds AJ, Oliver RF, Jahoda CA: Dermal cell populations show variable competence in epidermal cell support: Stimulatory effects of hair papilla cells. *J Cell Sci* 98:75–83, 1991

Reynolds AJ, Lawrence C, Cserhalmi-Friedman PB, Christiano AM, Jahoda CA: Trans-gender induction of hair follicles. *Nature* 402:33–34, 1999

Robinson M, Reynolds AJ, Gharzi A, Jahoda CA: *In vivo* induction of hair growth by dermal cells isolated from hair follicles after extended organ culture. *J Invest Dermatol* 117:596–604, 2001

Schaller SA, Li S, Ngo-Muller V, Han MJ, Omi M, Anderson R, Muneoka K: Cell biology of limb patterning. *Int Rev Cytol* 203:483–517, 2001

Stenn KS, Paus R: Controls of hair follicle cycling. *Physiol Rev* 81:449–494, 2001

Stenn KS, Lawrence L, Veis D, Korsmeyer S, Seiberg M: Expression of the bcl-2 protooncogene in the cycling adult mouse hair follicle. *J Invest Dermatol* 103:107–111, 1994

Tezuka M, Ito M, Ito K, Tazawa T, Sato Y: Investigation of germinative cells in generating and renewed anagen hair apparatus in mice using anti-bromodeoxyuridine monoclonal antibody. *J Dermatol Sci* 2:434–443, 1991

Tobin DJ, Hagen E, Botchkarev VA, Paus R: Do hair bulb melanocytes undergo apoptosis during hair follicle regression (catagen)? *J Invest Dermatol* 111:941–947, 1998

Uno H, Cappas A, Brigham P: Action of topical minoxidil in the bald stump-tailed macaque. *J Am Acad Dermatol* 16:657–668, 1987

Van Scott EJ, Ekel TM: Geometric relationships between the matrix of the hair bulb and its dermal papilla in normal and alopecic scalp. *J Invest Dermatol* 1:281–287, 1958

Weedon D, Strutton G: Apoptosis as the mechanism of the involution of hair follicles in catagen transformation. *Acta Derm Venereol* 61:335–339, 1981

Wessells NK, Roessner KD: Nonproliferation in dermal condensations of mouse vibrissae and pelage hairs. *Dev Biol* 12:419–433, 1965

Westgate GE, Messenger AG, Watson LP, Gibson WT: Distribution of proteoglycans during the hair growth cycle in human skin. *J Invest Dermatol* 96:191–195, 1991

Whiting DA: Possible mechanisms of miniaturization during androgenetic alopecia or pattern hair loss. *J Am Acad Dermatol* 45:S81–S86, 2001

Wolffe AP, Guschin D: Chromatin structural features and targets that regulate transcription. *J Struct Biol* 129:102–122, 2000